

Finding Needles in Haystacks: Scanning Tunneling Microscopy Reveals the Complex Reactivity of Si(100) Surfaces

Published as part of the *Accounts of Chemical Research* special issue “Microscopic Insights into Surface Catalyzed Chemical Reactions”.

Erik S. Skibinski and Melissa A. Hines*

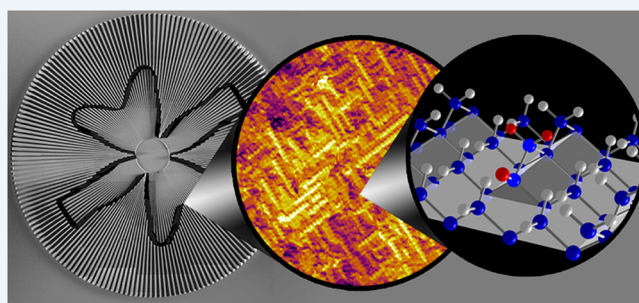
Department of Chemistry and Chemical Biology, Cornell University, Ithaca, New York 14853, United States

CONSPECTUS: Many chemical reactions—etching, growth, and catalytic—produce highly faceted surfaces. Examples range from the atomically flat silicon surfaces produced by anisotropic etchants to the wide variety of faceted nanoparticles, including cubes, wires, plates, tetrapods, and more. This faceting is a macroscopic manifestation of highly site-specific surface reactions. In this Account, we show that these site-specific reactions literally write a record of their chemical reactivity in the morphology of the surface—a record that can be quantified with scanning tunneling microscopy.

Paradoxically, the sites targeted by these highly site-specific reactions are extremely rare. This paradox can be understood from a simple kinetic argument. An etchant that produces atomically flat surfaces must rapidly etch every surface site *except* the terrace atoms on the perfectly flat surface. As a result, the etch morphology is dominated by the least reactive species (here, the terrace sites), not the most reactive species. In contrast, the most interesting chemical species—the site where the reaction occurs most rapidly and most selectively—is the hardest one to find. This highly reactive site, the key to the reaction, is the needle in the haystack, often occurring in densities far below 1% of a monolayer and thus invisible to surface spectroscopies. This kinetic argument is quite general and applies to a wide variety of reactions, not just etching reactions. Understanding these highly site-specific reactions requires a combination of experimental and computational techniques with both exquisite defect sensitivity and high chemical sensitivity.

In this Account, we present examples of highly site-specific chemistry on the technologically important face of silicon, Si(100). In one example, we show that the high reactivity of one particular surface site, a silicon dihydride bound to a silicon monohydride, or an “ α -dihydride”, provides a fundamental explanation for anisotropic silicon etching, a technology widely used in micromachining to selectively produce flat Si{111} surfaces. Fast-etching surfaces, such as Si(100) and Si(110), have geometries that support autocatalytic etching of α -dihydrides. In contrast, α -dihydrides exist only at kink sites on Si(111) surfaces. As a result, the etch rate of surfaces vicinal to Si(111) scales with the step density, approaching zero on the atomically flat surface. In a second example, we explain the chemistry that underlies pyramidal texturing of silicon wafers, a technique that is sometimes used to decrease the reflectivity of silicon solar cells. We show that a subtle change in chemical reactivity transforms a near-perfect Si(100) etchant into one that spontaneously produces nanoscale pyramids. The pyramids are not static features; they are self-propagating structures that evolve in size and location as the etching proceeds. The key to this texturing is the production of a very rare defect at the apex of each pyramid, a site that also etches autocatalytically.

These experiments show that simple chemical reactions can enable an exquisite degree of atomic-scale control if only we can learn to harness them.



INTRODUCTION

Every chemist dreams of watching a chemical reaction happen at the atomic scale, understanding why each of the atoms moves just so on its way from reactant to product. When scanning tunneling microscopy (STM) was invented in the early 1980s, surface science seemed to be halfway there. While the microscope was many orders of magnitude too slow for real-time reaction imaging, early STM images changed our perception of surface chemistry overnight. The ideal, perfectly flat single crystals that we imagined from our sharp diffraction patterns and clean Auger spectra were replaced by much less

perfect but strangely alluring landscapes covered by steps, pits, and protrusions, often in surprisingly regular patterns. What STM lacked in chemical sensitivity, it made up for in sheer beauty! But how could these pictures of little round balls be turned into rigorous, quantitative chemical insights?

The first quantitative experiments used detailed studies of equilibrium surfaces to quantify the relative energies of surface species, such as kinks and different types of steps. Many of

Received: March 19, 2015

Published: June 24, 2015

these analyses were inspired by the Wulff construction, which relates the equilibrium density of crystallographic facets to their relative energy. As an example, detailed images of meandering steps on annealed Si(100) surfaces were used to quantify the energies of step and kink sites on clean¹ and H-terminated surfaces.² Attention then turned to the subtle effects of strain on equilibrium and growth. Following the discovery that simply bending a silicon wafer leads to atomic-scale changes in terrace structure,^{3–5} researchers soon found that the strain inherent in heteroepitaxial growth leads to the spontaneous formation of hut clusters⁶ and nanowires.⁷

These experiments were very exciting but arguably more physics than chemistry. Could STM provide insights into “real” chemical reactions, the kind that happen in beakers? In some sense, the clean semiconductor surfaces favored by ultrahigh vacuum (UHV) surface science are exotic jewels, their dangling bonds far too reactive to survive in nature. In non-UHV environments, dangling bonds are rapidly passivated, which changes the surface reactivity dramatically.

This dichotomy is perhaps best illustrated by silicon. Since the dawn of the microelectronics era, surface scientists have known that clean and perfect Si surfaces are difficult to make and to preserve, as they react with the slightest contamination. In 1990, our view of these highly reactive surfaces was turned upside down when researchers at Bell Laboratories showed that a simple aqueous solution produced Si(111) surfaces that were not only almost atomically perfect, as shown in Figure 1a, but also stable in air for minutes to hours!⁸ The key was the passivating layer of H atoms.

In the mid-1990s, we^{9,10} and others^{11,12} set out to understand the reactions that produced atomically flat Si(111) and showed that the etching reactions literally write a record of their reactivity in the etched surface—a record that can be read with STM. One challenge was that there is no analogue of the Wulff construction for kinetic morphologies.

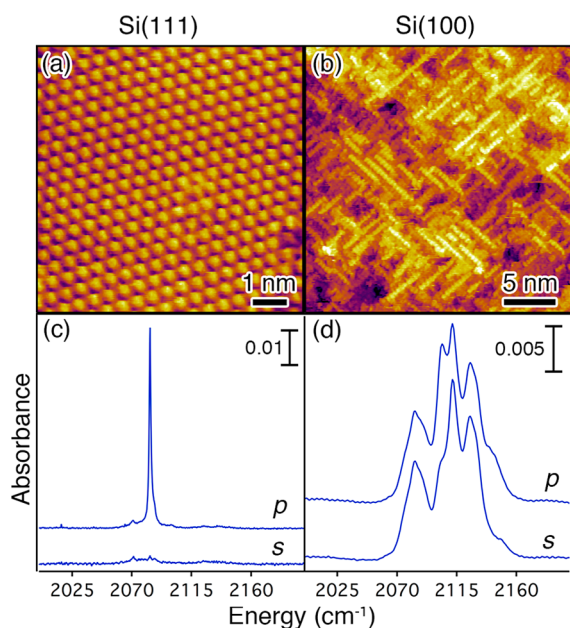


Figure 1. (a, b) STM images and (c, d) the Si–H stretch region of infrared spectra of NH₄F-etched Si(111) and Si(100). Although both surfaces are near-atomically flat, the H–Si(100) vibrational resonances are much broader and less strongly polarized than those of H–Si(111). The vertical scales are (a) 0.10 nm and (b) 4.27 nm.

The relative reactivity of the various surface sites, such as kinks and steps, cannot be directly inferred from the density of these species on the etched surface. We solved this problem with computer simulation. The bigger challenge is more subtle but can be understood from a simple argument. A chemical reaction that produces an atomically flat surface from a rough and bumpy surface must rapidly etch every surface species *except* the terrace atoms on the perfectly flat surface. As a result, a general feature of a steady-state etch morphology—here, the perfectly flat surface—is that it is dominated by the least reactive species, not the most reactive species. In contrast, the most interesting chemical species—the site where the reaction occurs most rapidly and most selectively—is the hardest one to find on an etched surface. This highly reactive site, the key to the etching reaction, is the needle in the haystack, typically occurring in densities far below 1% of a monolayer and thus invisible to surface spectroscopies.

The Si(111) surface is beloved by surface chemists for its simplicity. With a single “dangling” bond oriented normal to the surface (Figure 2), Si(111) comes close to embodying the

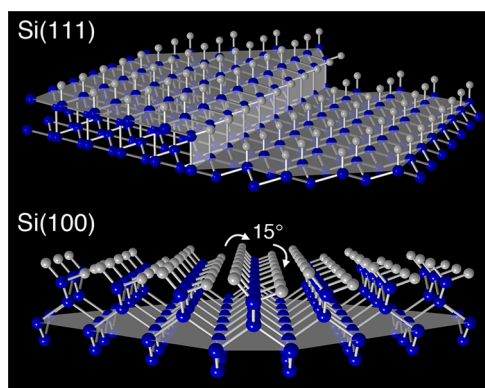


Figure 2. Molecular models of atomically flat H-terminated Si(111) and Si(100). The monohydride-terminated Si(111) surface is unstrained and experimentally observable. The atomically flat Si(100) surface has never been observed. Calculations suggest that dihydrides on flat Si(100) would be highly strained by interadsorbate interactions, leading them to cant by $\sim 15^\circ$ to relieve the strain. The gray and blue balls represent H and Si atoms, respectively.

step–ledge–kink model of growth (and etching) first proposed by Burton, Cabrera, and Frank in the 1950s.¹³ As a result, the most reactive site, the kink site, was not difficult to intuit from STM images of etched Si(111), and the relative reactivity of sites on the surface could be deduced primarily from step and pit morphologies.^{9,10}

The big question was whether the chemistry for making atomically flat Si(111) could be translated to Si(100). Outside of academia there is little interest in Si(111), as the microelectronics industry is based on Si(100). After a flurry of discouraging results in the early 1990s, conventional wisdom held that steric hindrance prevented the chemical production of atomically flat Si(100). If a perfectly flat Si(100) surface were terminated by the smallest possible atom, the H atoms on adjacent sites would be far too close, well within a van der Waals diameter. Indeed, first-principles calculations^{14,15} predicted that the atoms on a flat H-terminated surface would drastically cant by $\sim 15^\circ$ to partially relieve this strain, as shown in Figure 2. (While dimerized, monohydride-terminated Si(100)¹⁶ produced by high-temperature processing avoids

interadsorbate strain, dimerization has never been observed in aqueous processes.)

By the dawn of the 21st century, the quest for a chemical route to flat Si(100) was all but abandoned. The belief was that chemical etching would always progressively roughen a Si(100) surface, likely producing microfaceted, {111}-terminated asperities.

■ NEAR-ATOMICALLY PERFECT SI(100) AND AUTOCATALYTIC ETCHING OF α -DIHYDRIDES

Conventional wisdom was wrong: our inability to produce near-atomically flat Si(100) was not a problem of atomic-scale chemistry but rather a mesoscale effect. Most silicon etching reactions produce H₂ gas, which tends to collect on the etching surface, causing a variety of morphological irregularities.¹⁷ When this process is disrupted by pulling the sample through the etchant–air interface a few times per minute, the morphology of the etched surface is determined by atomic-scale effects. Under these conditions, when Si(100) is etched in 40% NH₄F(aq)—the same solution that produces atomically flat, H-terminated Si(111)—a near-atomically perfect H-terminated Si(100) surface is produced, as shown in Figure 1b.¹⁸

Why did it take almost 20 years to go from atomically flat Si(111) to near-atomically flat Si(100) if the same solution produces both surfaces? The answer lies in the infrared spectra of the surfaces, which are shown in Figure 1c,d. Few today remember that the production of atomically flat Si(111) was a triumph of spectroscopy, not microscopy.⁸ Every Si atom on an atomically flat Si(111) surface is terminated by an unstrained H atom oriented normal to the surface. As a result of this extreme homogeneity, the Si–H stretch vibration on atomically flat Si(111) has the narrowest line width of any covalently bonded surface adsorbate, only 0.1 cm⁻¹ at 130 K.¹⁹ This narrow line width, shown in Figure 1d, led the Bell Laboratories team to predict atomically flat surfaces long before STM images were available.⁸ The natural expectation was that an atomically (or near-atomically) flat H–Si(100) surface would have a similarly narrow line width, which is clearly not the case, as shown in Figure 1d. In the face of what appeared to be compelling spectroscopic evidence of rough Si(100) surfaces (i.e., broad infrared line widths), researchers soon gave up on the more challenging STM experiments, even though there are hints of near-flat Si(100) surfaces in the literature.²⁰

The unexpected production of near-atomically flat Si(100) opened up many questions. What was the chemical structure of the etched surface? Why was the infrared spectrum so broad? Most importantly, what chemical reaction caused these surfaces to form? Answering these questions required simultaneous advances in both spectroscopic and microscopic analysis.

Infrared spectroscopy had long indicated that the NH₄F-etched Si(100) surface is entirely H-terminated, but the broad spectral line widths made further analysis difficult. Originally, the broad and widely dispersed bands were attributed to a diversity of surface species, including silicon monohydrides, dihydrides, and trihydrides,²¹ but this assignment turned out to be inconsistent with the STM data, which revealed a relatively homogeneous morphology with no trihydrides.¹⁸

Suspecting that a simpler answer lay buried in the infrared spectroscopy, we dug more deeply into the polarization dependence of the spectra. The first issue is that absorption spectroscopy is typically performed with s- and p-polarized radiation. While s-polarized radiation can be aligned with a

principal crystallographic direction to simplify the spectrum, p-polarized radiation has both in-plane and out-of-plane components. As a result, p-polarized radiation cannot be aligned with a high-symmetry direction; it always has mixed character. To overcome this problem, we developed a mathematical technique that uniquely converts a set of spectra taken with both s- and p-polarized radiation into their Cartesian components,²² essentially the spectra that would be obtained with radiation polarized along the *x*, *y*, and *z* (surface normal) directions. By alignment of the Cartesian coordinates with the high-symmetry directions of the crystal, significant spectral simplification was achieved, albeit not enough to uniquely assign the spectrum.

Assigning the infrared spectrum of NH₄F-etched Si(100) required a second bit of luck. While a single Si(100) terrace has twofold rotational symmetry, the Si(100) surface has fourfold rotational symmetry by virtue of its alternating terrace structure. As a result, all infrared spectra taken with in-plane-polarized radiation on a flat Si(100) surface are identical regardless of azimuthal orientation; *x* cannot be distinguished from *y*. Inspired by the well-known step doubling and symmetry breaking on equilibrium vicinal Si(100) surfaces,²³ we investigated the NH₄F etching of vicinal Si(100), which also led to spontaneous symmetry breaking; *x* could be distinguished from *y*!

The combination of these two tricks, mathematical simplification and symmetry breaking, led to a dramatic simplification of the infrared spectrum of NH₄F-etched Si(100), as shown in Figure 3. In place of the nearly identical

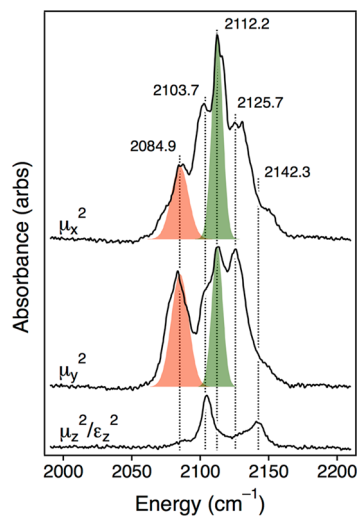


Figure 3. Cartesian components of the Si–H stretch region of the infrared spectrum of NH₄F-etched vicinal Si(100), with the five resolved bands indicated by dotted lines. The relative intensities of the shaded bands were used to quantify symmetry breaking on this surface.

spectra observed with s- and p-polarized radiation (Figure 1d), the full Cartesian analysis revealed the three-dimensional chemical structure of the etched surface. As described more fully in ref 18, four of the five vibrational bands could be uniquely assigned to the alternating row morphology shown in Figure 4. (Assignment of the fifth band required more information, as described in ref 24.) The long, atom-wide rows in the STM images were revealed to be rows of unstrained dihydrides with symmetric and antisymmetric Si–H stretch modes.²¹ The trenches between the atom-wide rows were

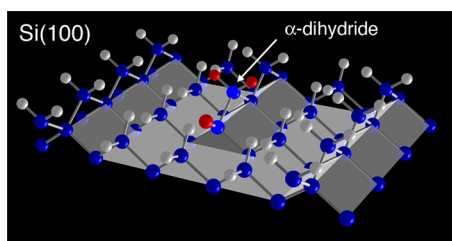


Figure 4. Molecular model of the alternating row morphology on Si(100) showing a row-end α -dihydride site. The elevated rows are terminated by unstrained dihydrides, whereas the trenches are terminated by strained dihydrides. The gray and blue balls represent H and Si, respectively.

found to be terminated with rows of strained dihydrides, which gave rise to independent vibrations of the upper and lower Si–H bonds on the dihydrides.¹⁵

Aided by the STM data, the infrared spectrum revealed the chemical structure of the NH_4F -etched surface but gave no insight into the mechanism of its formation. The interdigitated pattern of atom-wide etch features, visible in Figure 1b, had no obvious precedent in the literature. There was no analogue of the terrace–ledge–kink model of step-flow etching to guide analysis, and the identity of the fastest-etching site, the needle in the haystack, was unknown.

We tackled this problem with the only means at our disposal: brute force. The idea was to first simulate the morphologies that would result from all possible chemical reactivities and then to find the (hopefully unique) simulation that best matched experiment.²⁴

The first step was to define what was meant by “all possible chemical reactivities.” As chemists, we expected that different surface sites—sites with different chemical structures—would have different etch rates. The key was to find the minimum number of chemically distinct sites that would be necessary to reproduce experiment. For example, surface monohydrides, dihydrides, and trihydrides likely have dramatically different reactivities; however, simulations showed that this simple trichotomy could not account for the complex morphologies found experimentally.²⁵ A larger diversity of sites was necessary. Chemical intuition suggested that the mono-, di-, and trihydrides be further classified by local structural differences, such as steric hindrance and nearest-neighbor effects; however, a blind application of these two criteria would lead to hundreds of different surface sites—far too many for a brute force search.

Our analysis was aided by previous studies on the NH_4F etching of Si(111), which produced the atomically flat surfaces shown in Figure 1a. These experiments determined the etch rates of seven different sites, including the Si(111) terrace site and the well-known monohydride- and dihydride-terminated step sites on Si(111).^{9,10} These sites also exist on the Si(100) surface; however, the Si(111) studies provided little insight into the reactivity of dihydrides, the majority species on Si(100) surfaces. As described in ref 24, we parametrized the etch rates of the remaining sites with six free parameters. On the basis of this parametrization, the etch rate of every site on an arbitrary Si(100) surface was determined by the seven known etch rates and the six unknown parameters.

The next step was to generate a library of possible steady-state etch morphologies by varying each of the unknown parameters over 5–7 orders of magnitude and then simulating the removal of 50 monolayers of silicon from an initially flat

Si(100) surface and a similarly sized vicinal surface using kinetic Monte Carlo techniques.^{25,26} The final library contained 38 880 flat and 38 880 vicinal morphologies, with each pair of morphologies representing a unique combination of site-specific etch rates. A representative sampling of the simulated morphologies is shown in Figure 5.

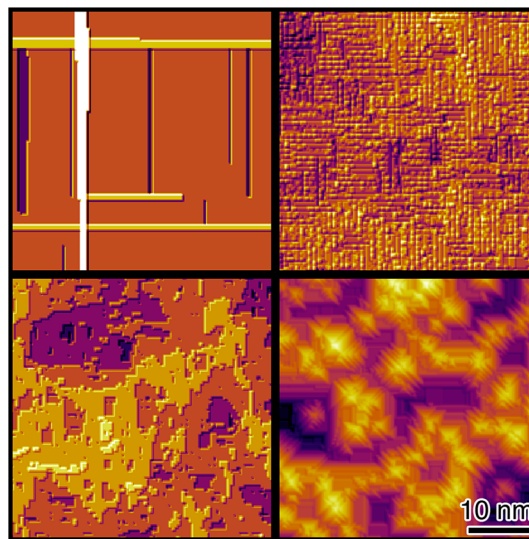


Figure 5. Representative morphologies from a library of simulated morphologies of Si(100) etching.

Which of these surfaces, if any, was the best fit to experiment? Our initial idea was to use pattern recognition technology to find the best visual match between experiment and simulation; however, this approach suffered from a number of complications, including the finite resolution of the experimental data. More importantly, this approach completely neglected the wealth of chemical information obtained from the spectroscopic measurements. For example, many simulations had single-atom-wide rows of elevated dihydrides, some with the dihydride parallel to the stripe and some with the dihydride perpendicular to the stripe. Morphologically, these rows are essentially identical, even though the infrared spectra were consistent only with the latter.

We took inspiration instead from the well-known *Calculus Eliminator* algorithm.²⁷ While it was difficult to find a single criterion that uniquely defined the best fit, it was relatively easy to identify multiple criteria that excluded large regions of the search space. In short, the key to finding the best match to the STM data was to first remove all of the simulations that were inconsistent with the spectroscopic data. As later research would show, this approach seems to be generally useful and not specific to this system.

For the case of NH_4F etching of Si(100), the most defining chemical aspect of the data was the symmetry breaking on etched vicinal surfaces. As described in ref 24, this symmetry breaking (or anisotropy) is readily quantified from polarized infrared spectroscopy. When simulations that differed by more than 20% from the measured anisotropy were eliminated, 99.87% of the library was removed from the search. Only 50 simulations remained! This subset was further culled by comparison to morphological data, such as the average length and density of single-atom-wide features. Figure 6 compares the experimental STM data to the best-fit simulated morphologies. This fit clearly identified the needle in the haystack—the most

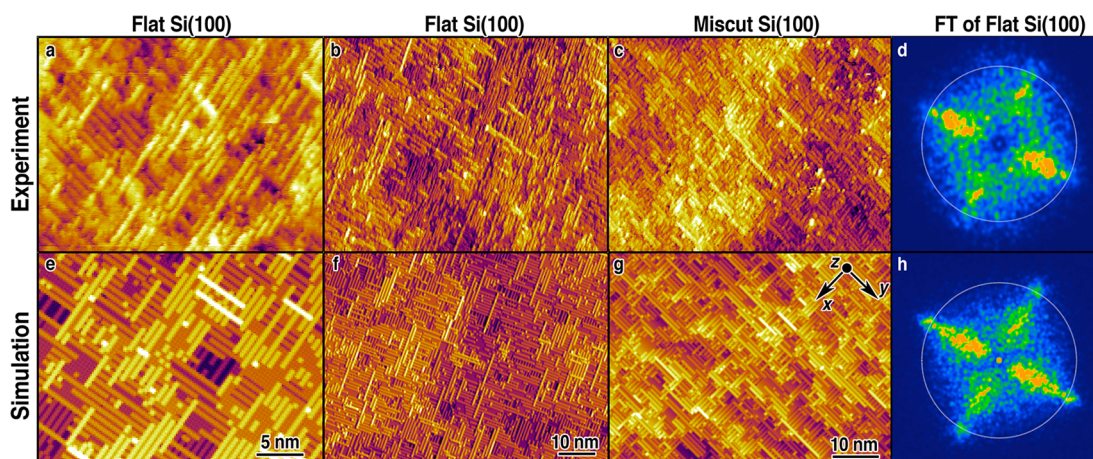


Figure 6. Comparison between experimental and best-fit simulated Si(100) morphologies. Experimental STM images of (a, b) flat and (c) vicinal NH_4F -etched Si(100) and (d) Fourier transform of the flat surface with the scale bar at 1.3 nm^{-1} corresponding to the alternating row morphology spacing. (e–h) Best-fit simulations of the experimental images. Reprinted from ref 24. Copyright 2012 American Chemical Society.

rapidly etching surface site—as a dihydride bound to (or “ α to”) an adjacent monohydride. We named these sites α -dihydrides. These species occur in a variety of locations but are typified by the row-end site shown in Figure 4.

Particularly in retrospect, the high reactivity of the α -dihydrides is easily understood. To remove an atom from the Si(100) surface, two backbonds to the surface must be cleaved. Simultaneous cleavage of both bonds is entropically disfavored, so the bonds must be broken sequentially. To avoid a tremendous energetic penalty, the first backbond must be broken *and passivated* prior to the second cleavage. In short, the first step of Si(100) etching must be an insertion reaction across a backbond, a reaction that is sterically challenging. Most dihydrides are directly backbonded to lattice sites and have limited flexibility. In contrast, α -dihydrides are bound to a monohydride species that can relax by pivoting around its two backbonds to the lattice in response to an insertion reaction. Therefore, the high reactivity of the α -dihydride is a direct consequence of steric hindrance.

The row-end α -dihydride has a particularly important role in the formation of near-atomically flat Si(100) because this site etches autocatalytically. Etching of a row-end α -dihydride creates a new α -dihydride of the adjacent dihydride. This autocatalytic behavior is directly responsible for the characteristic single-atom-wide rows, as seen in movies of the etching surface.²⁴

More importantly, autocatalysis of α -dihydrides provides a fundamental explanation for the anisotropic etching of silicon surfaces, a technology widely used in micromachining.²⁸ Engineers have long known that many basic solutions rapidly etch all silicon surfaces except Si{111}. As a result, these solutions can be used to selectively and precisely machine Si{111} surfaces for applications ranging from ink jet nozzles to nanoscale transistors. The key to this reactivity lies in the structure of silicon surfaces. Fast-etching surfaces, such as Si(100), Si(110), and their vicinal surfaces, have long (nominally infinite) rows that support autocatalytic α -dihydride etching. In contrast, the only α -dihydrides on Si(111) surfaces are kink sites on vicinal steps, as shown in Figure 7. As a result, the etch rates of surfaces vicinal to Si(111) scale with the step density, approaching zero on the flat surface.²⁹

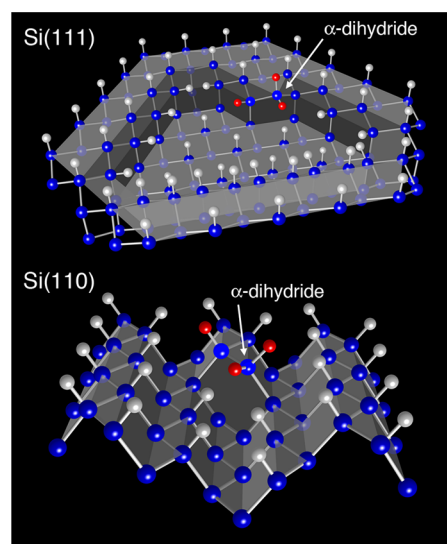


Figure 7. Molecular models of α -dihydride sites on Si(111) and Si(110). Si(110) surfaces etch very rapidly, as autocatalytic etching of α -dihydrides leads to self-propagating removal of infinite Si monohydride rows. In contrast, flat Si(111) surfaces etch very slowly, as pit growth is rate-limited by step-site etching, which nucleates two fast-etching kink sites (α -dihydrides). On vicinal Si(111) surfaces, the etch rate is expected to scale linearly with the step density, as observed experimentally.²⁹

■ ALTERNATING ROW MORPHOLOGY AND THE UNEXPECTED ROLE OF DIHYDRIDE STRAIN

One of the more surprising aspects of this “brute force” approach is that the chemical information sometimes encodes subtle morphological features—features that are not included in the search criteria. For example, the long atom-wide rows on the NH_4F -etched Si(100) surfaces have a notable preference for alternation, similar to the “missing row” reconstruction on certain transition-metal surfaces.³⁰ This leads to a secondary maximum in Fourier transforms of atomic-scale images, as shown in Figure 6. This preference for alternating rows is puzzling because it implies that the reaction preferentially removes every other row of atoms on the surface, even though all of the atoms on flat Si(100) are identical. Surprisingly, the best-fit morphologies show the same propensity toward

alternation, even though this propensity was not included in the search criteria.

The alternating row morphology is caused by an unexpected rate acceleration that is also driven by steric hindrance—a second needle in the haystack. On a perfectly flat Si(100) surface, all of the surface atoms are strained by the same amount. If one atom is removed from the surface, the atoms in the vicinity of the vacancy experience varying degrees of strain and distortion, as shown in Figure 8. The silicon atom closest

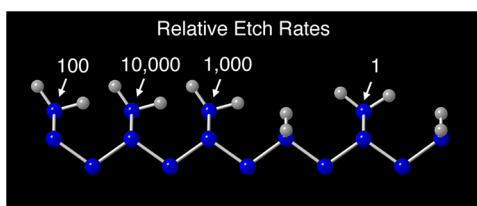


Figure 8. Molecular model of dihydrides on Si(100) showing the four different strain states used in etching simulations and their relative reactivities. The most reactive site is not the most strained site but rather the site whose etching leads to the most energy release by adjacent sites.

to the vacancy, although strained on only a single side, would relax toward the vacancy, leading to increased distortion. Similarly, the strained silicon atom adjacent to this relaxed site would be somewhat less strained than an atom on the ideal surface, although possibly more distorted. This type of position-dependent distortion has been seen in first-principles simulations but can also be explained by a simple mechanical model.²⁴

This type of position-dependent strain and distortion explains one of the most unexpected aspects of near-atomically flat Si(100): the broad infrared line shapes. The energy of the Si–H stretch vibration is sensitive to both interadsorbate stress¹⁵ and local changes in electronegativity.³¹ If every site on the surface were identical, the infrared spectrum would be characterized by extremely narrow vibrational resonances, as seen in the H/Si(111) system. The situation is different on Si(100) even though the morphology is near-atomically flat. Point defects on the near-atomically flat Si(100) surface lead to a wide range of strain states and distortions, with a single point defect affecting many sites in its vicinity. This heterogeneity is reflected in the broad infrared line shapes.

What effect do these varying degrees of strain and distortion have on the reactivity? The etching simulations revealed the unexpected reactivity pattern shown in Figure 8, where the fastest-etching site is neither the most strained nor the least strained site. Instead, the most reactive site is adjacent to the site that is strained on only one side. We attributed this acceleration to an unexpected manifestation of interadsorbate strain relief. Using a simple mechanical model of interadsorbate repulsion and structural distortion,²⁴ we showed that removing (etching) the most reactive site leads to more energy release by adjacent dihydrides than the removal of any other site. On this basis, we proposed that the energy stored in the interadsorbate strain helps drive the etching reaction over the activation barrier. This unusual dependence on interadsorbate strain leads to both the characteristic alternating row morphology and the dominance of single-atom-wide rows.

■ PYRAMIDAL TEXTURING AND THE AUTOCATALYTIC ETCHING OF α^2 -DIHYDRIDES

While atomically flat surfaces may be ideal for microelectronics, other applications require rough and bumpy surfaces. One example is photovoltaics, where chemical texturing is sometimes used to decrease the reflectivity of crystalline silicon, thereby enabling low-cost improvement in efficiency. This application makes use of the chance finding that some silicon etchants transform flat Si(100) wafers into surfaces covered with micron-scale Si{111}-terminated pyramids. Unfortunately, this process suffers from reproducibility issues. Fresh etchant often requires an induction period before texturing begins, whereas old etchant can unexpectedly stop working. Process improvements have been stymied by a simple problem: the chemical and physical origins of pyramidal faceting are unknown. While many basic etchants produce atomically flat Si(111), only a subset of these etchants cause pyramidal faceting on Si(100).

The key to understanding the faceting transition was to find a surface that produced both faceted and nonfaceted regions, such as the H₂O-etched Si(100) surface shown in Figure 9.^{32,33} In this case, both the steady-state morphology and the infrared spectrum were complex; both contained some incontrovertible information, but neither was readily assignable in its entirety. The well-resolved H–Si(111) and H–Si(100) transitions in the

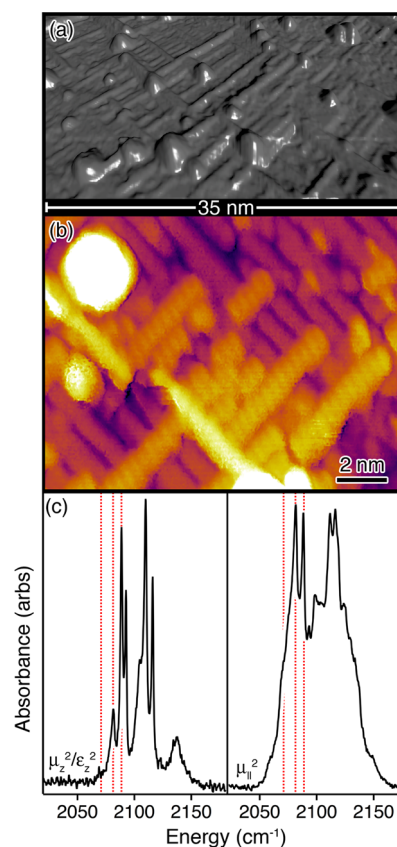


Figure 9. Pyramidal texturing of Si(100) by H₂O etching. (a) The rendered STM image shows {111}-faceted pyramids and elevated stripes, whereas (b) the high-resolution STM image reveals regions of alternating row morphology. The elliptical protrusions correspond to individual dihydrides. (c) The Si–H stretch region of the infrared spectrum shows many vibrational modes. The dashed red lines indicate modes attributed to Si{111} and Si{110} nanofacets.

infrared spectra and the faceted protrusions in the rendered STM images provided definitive evidence of pyramidal faceting, whereas high-resolution STM images (and the infrared spectra) showed the development of the alternating row morphology characteristic of NH_4F -etched $\text{Si}(100)$ surfaces. The elevated “stripes” that were often found connecting two pyramids were more confusing. Although early studies suggested that the stripes were dihydride-terminated,³² high-resolution images, such as in Figure 9, failed to resolve the expected elliptical protrusions along the tops of the stripes.³³

Our first approach was to search the original library of simulated $\text{Si}(100)$ morphologies for candidate matches. Casting a wide net, we searched for morphologies with $\geq 5\%$ of a monolayer of $\text{Si}\{111\}$, $\geq 5\%$ of a monolayer of $\text{Si}\{110\}$, and a significant coverage of the alternating row morphology (i.e., morphologies containing near-equal densities of strained and unstrained dihydrides). To our surprise, no such morphologies existed in the original library. Our model was incomplete; it did not distinguish among a sufficiently diverse set of sites.

Prior research on pyramidal faceting in two and three dimensions had emphasized the importance of the pyramid apex site.^{34–36} If this site is too reactive, the pyramid etches away as soon as it forms, but below a certain maximum reactivity, the apex site stabilizes pyramids. Although the pyramid apex could not be directly imaged, molecular models of $\text{Si}\{111\}$ -faceted pyramids suggested that the pyramids were terminated by a single unstrained dihydride bound to two monohydrides on opposing faces, a site we termed the α^2 -dihydride. Could this be the needle in this haystack?

To investigate the possibility of α^2 -dihydride-stabilized pyramids, we expanded the original library to include cases where α^2 -dihydrides were less reactive than α -dihydrides. (The original library assumed that the reactivities of α - and α^2 -dihydrides were identical.) When the expanded library was searched, a number of candidate morphologies emerged. The best-fit morphology, shown in Figure 10, was then obtained by comparing the experimental and simulated hillock densities. While the pyramids appear to be somewhat larger in experiment than in simulation, this discrepancy is due to tip convolution.

The images in Figure 10 belie the complexity of the texturing process. The pyramids are not static features; they are self-

propagating structures that evolve in size and location, as demonstrated by movies of the etching simulations.³³ Etching of the flat $\text{Si}(100)$ surface causes adjacent pyramids to increase in height, whereas etching of the $\text{Si}\{111\}$ faces or the α^2 -dihydride apex causes the pyramids to shrink. On average, these two processes balance one another, leading to a characteristic pyramid height. In a manner analogous to the propagation of α -dihydrides on the NH_4F -etched $\text{Si}(100)$ surface, the etching of an α^2 -dihydride site leads to the generation of a new α^2 -dihydride at an adjacent site. In this sense, pyramidal texturing is also autocatalytic.

Perhaps most interestingly, the simulations show that the reactivity of a single site, the α^2 -dihydride, which is present at a concentration of less than 0.4% of a monolayer, controls kinetic faceting. This observation has profound implications for surface chemistry, as it shows yet again that a spectroscopically invisible species controls the structure of the etching surface.

■ IMPLICATIONS AND FUTURE PROSPECTS

In this Account, we have presented a number of examples of highly site-specific silicon chemistry in which the most reactive site on the etching surface was present in concentrations far too low to be observed spectroscopically. Conversely, the most abundant sites on these surfaces, the sites that were most easily detectable, were essentially unreactive. Understanding the complicated reactivity of these surfaces required a combination of experimental and computational techniques with both exquisite defect sensitivity and high chemical sensitivity.

The big question is whether this reactivity pattern is a general trend or an anomaly. Recently we have shown that this selectivity is not restricted to silicon but also extends to metal oxides.³⁷ In our opinion, this pattern is much more general, as many chemical reactions—etching, growth, and catalytic—are known to produce highly faceted surfaces. As argued in the Introduction, faceting is a macroscopic manifestation of highly site-specific reactions. In particular, the wide range of nanoparticle shapes and structures that have been synthesized in the past decade—from cubes to wires to plates to tetrapods and more—suggest that simple chemistry can enable an exquisite degree of atomic-scale control if only we can learn to harness it.

■ AUTHOR INFORMATION

Corresponding Author

*E-mail: Melissa.Hines@cornell.edu.

Notes

The authors declare no competing financial interest.

Biographies

Erik S. Skibinski received his B.S. in chemistry from SUNY Geneseo in 2012 and is now a graduate student at Cornell University. His current research focuses on surface chemistry and methods of controlling semiconductor surfaces with simple chemical processes.

Melissa A. Hines earned an S.B. in chemistry from MIT in 1984 and a Ph.D. in chemistry from Stanford University in 1992. After postdoctoral research at AT&T Bell Laboratories in Murray Hill, NJ, she joined the Cornell University faculty in 1994. Her research interests include chemical etching, semiconductor surface chemistry, nanoscale surfaces, and the mechanical properties of nanoscale materials.

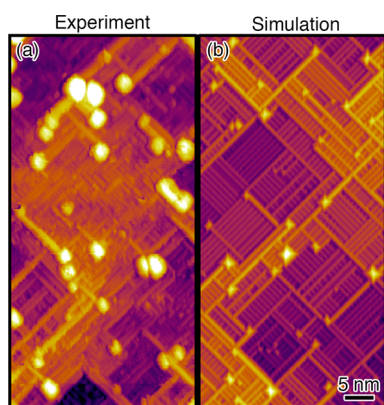


Figure 10. Comparison of (a) experimental and (b) best-fit simulated H_2O -etched $\text{Si}(100)$ morphologies. Tip convolution increases the apparent size of the pyramids in the experimental images. The pyramid densities are (a) $1.95 \times 10^{12} \text{ cm}^{-2}$ and (b) $1.72 \times 10^{12} \text{ cm}^{-2}$ in experiment and simulation, respectively.

ACKNOWLEDGMENTS

The work on Si(100) would not have been possible without the contributions of many talented students, including Marc F. Faggin, Brandon A. Aldinger, Ankush Gupta, and Ian T. Clark. This work was supported by the National Science Foundation (NSF) under Award CHE-1303998 and made use of shared facilities supported through the NSF MRSEC Program (DMR-1120296). E.S.S. was supported by the NSF IGERT Program (DGE-0903653).

REFERENCES

- (1) Swartzentruber, B. S.; Mo, Y.-W.; Kariotis, R.; Lagally, M. G.; Webb, M. B. Direct Determination of Step and Kink Energies on Vicinal Si(001). *Phys. Rev. Lett.* **1990**, *65*, 1913–1916.
- (2) Laracuenta, A. R.; Whitman, L. J. Step Structure and Surface Morphology of Hydrogen-Terminated Silicon: (001) to (114). *Surf. Sci.* **2003**, *545*, 70–84.
- (3) Webb, M. B.; Men, F. K.; Swartzentruber, B. S.; Kariotis, R.; Lagally, M. G. Surface Step Configurations under Strain: Kinetics and Step–Step Interactions. *Surf. Sci.* **1991**, *242*, 23–31.
- (4) Swartzentruber, B. S.; Kitamura, N.; Lagally, M. G.; Webb, M. B. Behavior of Steps on Si(001) as a Function of Vicinality. *Phys. Rev. B* **1993**, *47*, 13432–13441.
- (5) Jones, D. E.; Pelz, J. P.; Xie, Y. H.; Silverman, P. J.; Gilmer, G. H. Enhanced Step Waviness on SiGe(001)-(2 × 1) Surfaces under Tensile Strain. *Phys. Rev. Lett.* **1995**, *75*, 1570–1573.
- (6) Mo, Y.-W.; Savage, D. E.; Swartzentruber, B. S.; Lagally, M. G. Kinetic Pathway in Stranski–Krastanov Growth of Ge on Si. *Phys. Rev. Lett.* **1990**, *65*, 1020–1023.
- (7) Tersoff, J.; Tromp, R. M. Shape Transition in Growth of Strained Islands: Spontaneous Formation of Quantum Wires. *Phys. Rev. Lett.* **1993**, *70*, 2782–2785.
- (8) Higashi, G. S.; Chabal, Y. J.; Trucks, G. W.; Raghavachari, K. Ideal Hydrogen Termination of the Si(111) Surface. *Appl. Phys. Lett.* **1990**, *56*, 656–658.
- (9) Hines, M. A. The Picture Tells the Story: Using Surface Morphology To Probe Chemical Etching Reactions. *Int. Rev. Phys. Chem.* **2001**, *20*, 645–672.
- (10) Hines, M. A. In Search of Perfection: Understanding the Highly Defect-Selective Chemistry of Anisotropic Etching. *Annu. Rev. Phys. Chem.* **2003**, *54*, 29–56.
- (11) Kasparian, J.; Elwenspoek, M.; Allongue, P. Digital Computation and in Situ STM Approach to Silicon Anisotropic Etching. *Surf. Sci.* **1997**, *388*, 50–62.
- (12) Zhou, H.; Fu, J.; Silver, R. M. Time-Resolved Kinetic Monte Carlo Simulation Study on Si(111) Etching. *J. Phys. Chem. C* **2007**, *111*, 3566–3574.
- (13) Burton, W. K.; Cabrera, N.; Frank, F. C. The Growth of Crystals and the Equilibrium Structure of Their Surfaces. *Philos. Trans. R. Soc., A* **1951**, *243*, 299–358.
- (14) Northrup, J. E. Structure of Si(100)H: Dependence on the H Chemical Potential. *Phys. Rev. B* **1991**, *44*, 1419–1422.
- (15) Freking, U.; Krüger, P.; Mazur, A.; Pollmann, J. Surface Phonons of Si(001)-(1 × 1) Dihydride. *Phys. Rev. B* **2004**, *69*, No. 035315.
- (16) Chabal, Y. J.; Raghavachari, K. Surface Infrared Study of Si(100)-(2 × 1)H. *Phys. Rev. Lett.* **1984**, *53*, 282–285.
- (17) Aldinger, B. S.; Clark, I. T.; Gupta, A.; Hines, M. A. The Same Etchant Produces Both Near-Atomically Flat and Microfaceted Si(100) Surfaces: The Effects of Gas Evolution on Etch Morphology. *J. Appl. Phys.* **2010**, *107*, No. 103520.
- (18) Clark, I. T.; Aldinger, B. S.; Gupta, A.; Hines, M. A. Aqueous Etching Produces Si(100) Surfaces of Near-Atomic Flatness: Stress Minimization Does Not Control Morphology. *J. Phys. Chem. C* **2010**, *114*, 423–428.
- (19) Dumas, P.; Chabal, Y. J.; Higashi, G. S. Coupling of an Adsorbate Vibration to a Substrate Surface Phonon: H on Si(111). *Phys. Rev. Lett.* **1990**, *65*, 1124–1127.
- (20) Morita, Y.; Tokumoto, H. Atomic Scale Flattening and Hydrogen Termination of the Si(001) Surface By Wet-Chemical Treatment. *J. Vac. Sci. Technol., A* **1996**, *14*, 854–858.
- (21) Chabal, Y. J.; Higashi, G. S.; Raghavachari, K.; Burrows, V. A. Infrared Spectroscopy of Si(111) and Si(100) Surfaces: Hydrogen Termination and Surface Morphology. *J. Vac. Sci. Technol., A* **1989**, *7*, 2104–2109.
- (22) Clark, I. T.; Aldinger, B. S.; Gupta, A.; Hines, M. A. Extracting Maximum Information from Polarized Surface Vibrational Spectra: Application to Etched, H-Terminated Si(110) Surfaces. *J. Chem. Phys.* **2008**, *128*, No. 144711.
- (23) Alerhand, O. L.; Berker, A. N.; Joannopoulos, J. D.; Vanderbilt, D.; Hamers, R. J.; Demuth, J. E. Finite-Temperature Phase Diagram of Vicinal Si(100) Surfaces. *Phys. Rev. Lett.* **1990**, *64*, 2406–2409.
- (24) Hines, M. A.; Faggin, M. F.; Gupta, A.; Aldinger, B. S.; Bao, K. Self-Propagating Surface Reactions Produce Near-Ideal Si(100) Surfaces. *J. Phys. Chem. C* **2012**, *116*, 18920–18929.
- (25) Gupta, A.; Aldinger, B. S.; Faggin, M. F.; Hines, M. A. Kinetic Monte Carlo Simulations of Anisotropic Si(100) Etching: Modeling the Chemical Origins of Characteristic Etch Morphologies. *J. Chem. Phys.* **2010**, *133*, No. 044710.
- (26) Flidr, J.; Huang, Y.-C.; Newton, T. A.; Hines, M. A. Extracting Site-Specific Reaction Rates from Steady State Surface Morphologies: Kinetic Monte Carlo Simulations of Aqueous Si(111) Etching. *J. Chem. Phys.* **1998**, *108*, 5542–5553.
- (27) Seuss, Dr. *The Cat in the Hat (Television Broadcast)*; Pratt, H., Dir.; CBS Productions: Los Angeles, CA, 1971.
- (28) Elwenspoek, M.; Jansen, H. V. *Silicon Micromachining*; Cambridge University Press: Cambridge, U.K., 2004.
- (29) Wind, R. A.; Hines, M. A. Macroscopic Etch Anisotropies and Microscopic Reaction Mechanisms: A Micromachined Structure for the Rapid Assay of Etchant Anisotropy. *Surf. Sci.* **2000**, *460*, 21–38.
- (30) Ho, K.-M.; Bohnen, K. P. Stability of the Missing-Row Reconstruction on FCC (110) Transition-Metal Surfaces. *Phys. Rev. Lett.* **1987**, *59*, 1833–1836.
- (31) Lucovsky, G. Relation of Si–H Vibrational Frequencies to Surface Bonding Geometry. *J. Vac. Sci. Technol.* **1979**, *16*, 1225–1228.
- (32) Faggin, M. F.; Green, S. K.; Clark, I. T.; Queeney, K. T.; Hines, M. A. Production of Highly Homogeneous Si(100) Surfaces by H₂O Etching: Surface Morphology and the Role of Strain. *J. Am. Chem. Soc.* **2006**, *128*, 11455–11462.
- (33) Skibinski, E. S.; Hines, M. A. Molecular Mechanism of Etching-Induced Faceting on Si(100): Micromasking Is Not a Prerequisite for Pyramidal Texturing. *J. Phys. Chem. C* **2014** DOI: 10.1021/jp5063385.
- (34) Flidr, J.; Huang, Y.-C.; Hines, M. A. An Atomistic Mechanism for the Production of Two- and Three-Dimensional Etch Hillocks on Si(111) Surfaces. *J. Chem. Phys.* **1999**, *111*, 6970–6981.
- (35) Gosálvez, M. A.; Nieminen, R. M. Surface Morphology during Anisotropic Wet Chemical Etching of Crystalline Silicon. *New J. Phys.* **2003**, *5*, No. 100.
- (36) Mirabella, D. A.; Suárez, M. P.; Aldao, C. M. Hillock Sizes after Wet Etching in Silicon. *Surf. Sci.* **2009**, *603*, 3346–3349.
- (37) Song, A.; Jing, D.; Hines, M. A. Rutile Surface Reactivity Provides Insight into the Structure-Directing Role of Peroxide in TiO₂ Polymorph Control. *J. Phys. Chem. C* **2014**, *118*, 27343–27352.